Optica Applicata, Vol. XXXII, No. 4, 2002

Laser polarization visualization and selection of biotissue images

OLEG V. ANGELSKY, ALEXANDER G. USHENKO, DIMITRY N. BURKOVETS, YURIY A. USHENKO

Department of Correlation Optics, University of Chernivtsi, Kotsyubinsky Str. 2, 58012 Chernivtsi, Ukraine.

This paper is devoted to the analysis and experimental testing of the concept of laser polarization biotissue probing. The methods of increasing the signal-to-noise ratio in coherent images of the optically anisotropic architectonics of the morphological biotissue structure are considered. The possibilities of polarization selection and contrasting of such images screened by other biotissues are examined. The influence of the depolarization degree of the scattered background on the signal -to-noise ratio is investigated. The possibilities of polarization correction of the probing beam for contrasting biotissue images are analyzed.

1. Introduction

Until recently, the vector nature of radiation scattered by biotissues was usually ignored. Apparently, such an attitude was adopted due to the random character of turbid media and analysis of the scattered radiation field showing fast depolarization. However, in certain cases (low-density eye biotissues, cell monolayers, surface skin layers, *etc.*), the polarization degree of transmitted or reflected light becomes essentially nonzero and can be easily measured. Therefore, it would be important to extend the theoretical and experimental background of the studies of optical properties of biotissues using polarized light. At least two approaches can be distinguished. First, it might be important to expand our understanding of the transformation of polarized radiation by biotissues using the formalism of the Stokes vector and the Müller matrix. The second urgent task is to analyze the vector structure of random laser fields aimed at subsequent development of methods for the polarization selection of such fields.

The first studies devoted to the depolarization degree of laser radiation have revealed the sensitivity of this parameter to the type and the physiological state of a biotissue, which may be important for the diagnostics of pathological changes in biotissues.

It was shown experimentally that the light propagating in such a strongly scattering object as skin retains its linear polarization within millimeter depths. Such an optical path in a biotissue allows macroinhomogeneities in biotissues to be imaged with the use of polarization methods. Specifically, TUCHIN [1] has experimentally demonstrated the possibility of visualizing microvessels in face skin by using the vector analysis of face skin images with subsequent polarization contrasting.

This paper is aimed at studying the possibilities of using polarization methods to improve the signal-to-noise ratio in images of optically anisotropic structures (collagen and myosin networks, hematomas, neoplasm, *etc.*) in the case where the biotissue being probed is screened by another biotissue. We will consider two situations: singly and multiply scattering object scenes.

2. Single scattering

2.1. Theoretical modeling

The field of laser radiation scattered by a singly scattering bioobject can be generally represented as a sum of two terms

$$I = I^* + \tilde{I} \tag{1}$$

where I^* and $\tilde{I}$ are the intensities of the informative and background components of the signal, respectively.

The components involved in Eq. (1) can be generally represented in the form of the following functionals [2], [3]:

$$I^* = \Psi(\{x_{ik}[\rho_x, \sigma_x(\Delta n_x)]\}),$$

$$\tilde{I} = T(\{y_{ik}[\rho_y, \sigma_y(\Delta n_y)]\}). \tag{2}$$

Here, Ψ and T are the algorithms (the generalized Malus law) for determining the intensity of elliptically polarized radiation [2] and $\{x_{ik}(\rho, \Delta n)\}$ and $\{y_{ik}(\rho, \Delta n)\}$ are the elements of Müller matrices [3] determined by the orientation ρ and anisotropy Δn of architectonic structures of biotissues.

Applying the vector-parametric description of light fields [3], we can demonstrate that the operation of polarization selection ("suppression" of the background signal intensity) leads to the following improvement of the signal-to-noise ratio for an image of a biotissue screened by another light-scattering medium

$$\eta = \frac{I^* + (I^* + \tilde{I})\mu}{\tilde{I} + (I^* + \tilde{I})\mu} = \frac{I^* + \tilde{I}\dfrac{\mu}{\mu + 1}}{\tilde{I} + I^*\dfrac{\mu}{\mu + 1}} \tag{3}$$

where:

$$I^* = \sin^2\left[\arctan\left(\frac{G^* - W^*}{1 + G^*W^*}\right)\right] + \cos^2\left[\arctan\left(\frac{G^* - W^*}{1 + G^*W^*}\right)\right]\tan^2 J^*, \tag{4}$$

$$\tilde{I} = \sin^2\left[\arctan\left(\frac{G^* - W^*}{1 + G^*W^*}\right)\right] + \cos^2\left[\arctan\left(\frac{G^* - W^*}{1 + G^*W^*}\right)\right]\tan^2 \tilde{J}, \tag{5}$$

$$J^* = 0.5\arcsin(x_{42}\cos 2\alpha_0\cos 2\beta_0 + x_{43}\cos 2\alpha_0\cos 2\beta_0 + x_{44}\sin 2\beta_0), \quad (6)$$

$$\tilde{J} = 0.5\arcsin(y_{42}\cos 2\alpha_0\cos 2\beta_0 + y_{43}\cos 2\alpha_0\cos 2\beta_0 + y_{44}\sin 2\beta_0), \quad (7)$$

$$G^* = \frac{x_{32}\cos 2\alpha_0\cos 2\beta_0 + x_{33}\cos 2\alpha_0\cos 2\beta_0 + x_{34}\sin 2\beta_0}{x_{22}\cos 2\alpha_0\cos 2\beta_0 + x_{23}\cos 2\alpha_0\cos 2\beta_0 + x_{24}\sin 2\beta_0}, \quad (8)$$

$$W^* = \frac{y_{32}\cos 2\alpha_0\cos 2\beta_0 + y_{33}\cos 2\alpha_0\cos 2\beta_0 + y_{34}\sin 2\beta_0}{y_{22}\cos 2\alpha_0\cos 2\beta_0 + y_{23}\cos 2\alpha_0\cos 2\beta_0 + y_{24}\sin 2\beta_0}. \quad (9)$$

Here, $\mu \approx 10^3$ is the coefficient that determines the linearity degree of the polarization analyzer; α_0 and β_0 are the azimuth and the ellipticity of the polarization of the probing laser beam, respectively; $\arctan[(G^* - W^*)/(1 + G^*W^*)] = \Delta\alpha$ is the difference of the azimuthal angles of polarization vectors of the background and object signals; J^*, $\tilde{J}$ are the ellipticities of these signals.

Analysing of Eqs. (4)–(9) it can be seen that the optimal situation for the polarization improvement of the signal-to-noise ratio is determined by the following boundary conditions:

$$\left[\arctan\left(\frac{G^* - W^*}{1 + G^*W^*}\right)\right] \to \frac{\pi}{2}, \quad J^* \to \frac{\pi}{4}, \quad \tilde{J} \to 0. \quad (10)$$

On the other hand, the improvement factor of the signal-to-noise ratio is a multiparametric function of polarization angles (α_0, β_0) (Θ is the angle of light scattering measured from the normal to the biotissue surface) and optical parameters of the object scene

$$\eta \equiv \Omega\{\alpha_0, \beta_0, x_{ik}[\rho_x, \delta_x(\Delta n_x)], y_{ik}[\rho_y, \delta_y(\Delta n_y)], \Theta\}. \quad (11)$$

Let us consider the possibilities of improving the signal-to-noise ratio in the case where a singly scattering optically anisotropic biotissue structure is probed with a linearly polarized laser beam (α_0, = 0°–90°, β_0 = 0°).

For simplicity, we can assume without loss of the generality of our consideration that the biotissue being diagnosed and the screening tissue have a quasi-structured architectonics. In other words, the variance of orientations of elements (fibers) in the architectonic network [4]–[6] is sufficiently small $\sigma_\rho \to 0°$. This class of object scenes includes such biosystems as "layers of fibrillar muscular tissue", "sinew–muscular tissue", "muscle–bony tissue", "connective tissue–muscle", *etc.*

2.2. Computer modeling, analysis, and discussion

Figure 1 presents the results of computer modeling of the "spatial" (Figs. 1**a**, **b**) and "topological" (Figs. 1**c**, **d**) distributions of the coefficient $\eta(\alpha_0, \Theta)$ for an object scene with the following parameters: Δn_x = 0.1; Δn_y = 0.03 (Figs. 1**a**, **c**) and 0.08

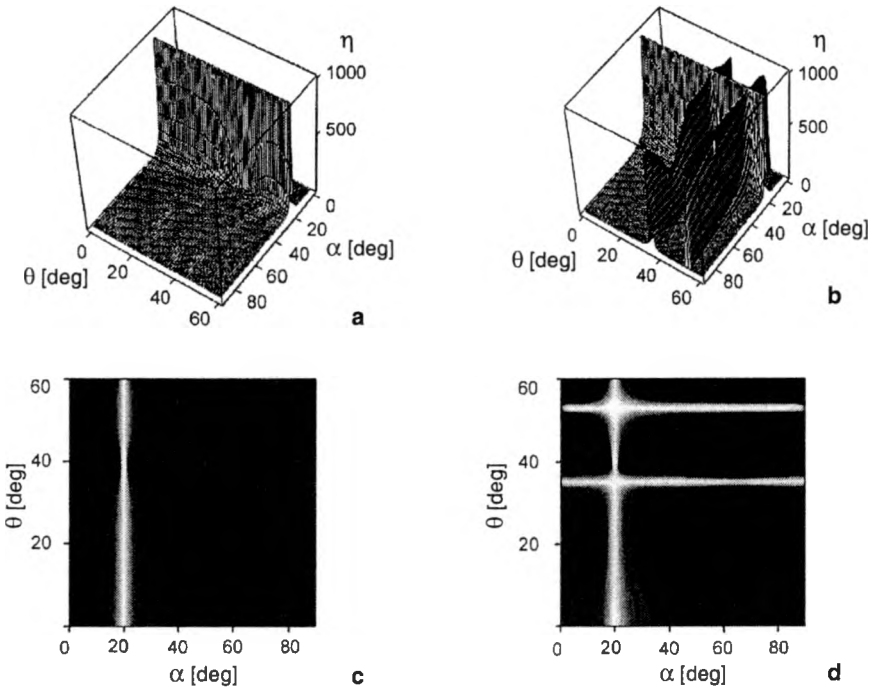

Fig. 1. Spatial-azimuthal and topological dependences of the improvement factor of the signal-to-noise ratio.

(Figs. 1**b**, **d**), and $\Delta\rho = \rho_x - \rho_y = 20°$. The results of these calculations allow us to make the following conclusions:

– The efficiency of polarization selection of the informative signal is highly sensitive to the azimuthal geometry of probing. The coefficient $\eta(\alpha_0, \Theta)$ has a rather complicated topological distribution, and the value of this coefficient ranges from 0 to μ.

– The extremal level of $\eta(\alpha_0, \Theta)$ for all the angular arrangements is localized around the azimuthal angle of polarization of the probing beam $\alpha_0 = \Delta\rho$.

– The decrease in the difference of anisotropy levels (Δn_x and Δn_y) in biotissues is accompanied by the formation of additional extrema $\{\eta(\alpha_0, \Theta)\}\big|_{\Theta_i = \text{const}}$ for all the values of azimuthal angles α_0.

Let us analyze these results. As it follows from boundary conditions (10), the extreme increase in the signal-to-noise ratio is achieved when the background signal is linearly polarized. In this case, the intensity of the background signal can be reduced to the level of $\tilde{J} \times \mu^{-1}$. Such a background suppression is achieved when the azimuth α_0 coincides with the anisotropy direction ρ_y of screening biotissue (this direction is measured from ρ_x), *i.e.*, $\alpha_0 = \Delta\rho$. Thus, an extremum line should exist in the distribution $\eta(\alpha_0, \Theta)$ for all the scattering angles Θ.

On the other hand, Eqs. (6)–(9) show that the level of the background and informative signals considerably depends on the relations between the partial matrix

elements $\{x_{ik}\}$ and $\{y_{ik}\}$. The values of these elements fluctuate in different ways, depending on anisotropy parameters Δn_x, Δn_y, and angle Θ [3]. Therefore, a linearly polarized background and the relevant extremum lines $\{\eta(\alpha_0, \Theta)\}|_{\Theta_i = \text{const}}$ may be observed within a broad range of α_0 (Figs. 1**b**, **d**).

Figure 2 displays the dependences characterizing the transformation of the polarization structure of the background $\tilde{I}$ and informative I^* signals in response to variations in the azimuth α_0 of the probing beam. These results were obtained for the following scattering angles: $\Theta = 0°$ (Figs. 2**a**, **d**), $\Theta = 35°$ (Figs. 2**b**, **e**), and $\Theta = 55°$ (Figs. 2**c**, **f**). The left-hand column corresponds to anisotropy parameters $\Delta n_x = 0.1$ and $\Delta n_y = 0.03$, while the right-hand column corresponds to anisotropy parameters $\Delta n_x = 0.1$ and $\Delta n_y = 0.08$.

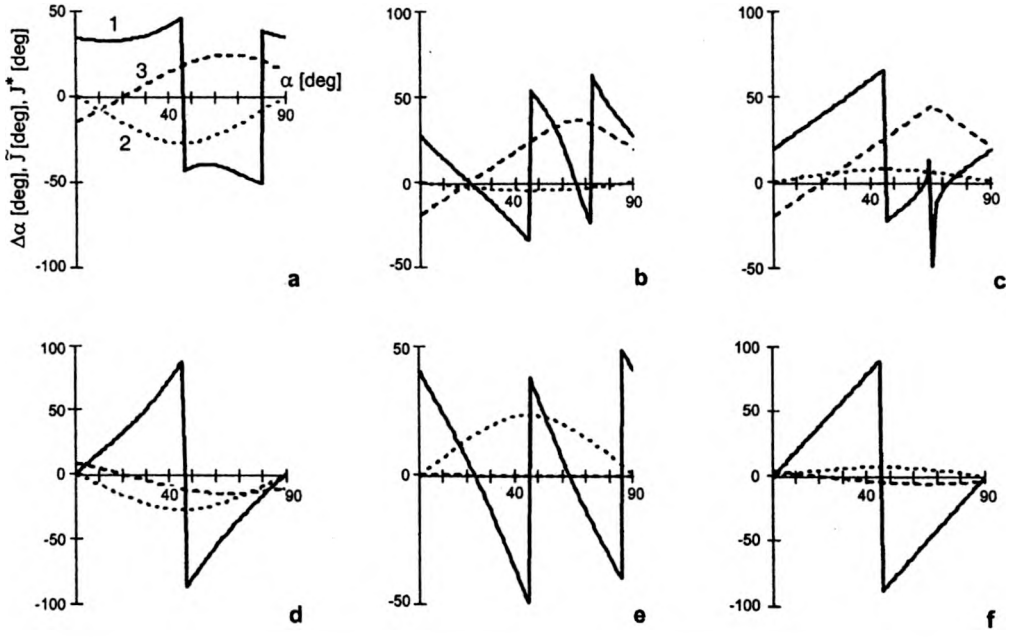

Fig. 2. Polarization structure of the background and informative signals: **a** – $\theta = 0°$, **b** – $\theta = 35°$, **c** – $\theta = 55°$, **d** – $\theta = 0°$, **e** – $\theta = 35°$, **f** – $\theta = 55°$; (1 – $\Delta\alpha$, 2 – J^*, 3 – $\tilde{J}$).

The analysis of these data reveals a correlation between zero values of the ellipticity of the background signal (curves 3) and the extreme level of the improvement factor of the signal-to-noise ratio $\eta(\alpha_0, \Theta) \to \mu$, which is observed for arbitrary values of polarization parameters of the informative signal $\arctan[(G^* - W^*)/(1 + G^*W^*)] = \Delta\alpha$ and J^* (curves 1 and 2).

For other values of the azimuthal angle α_0 of polarization of the probing beam, two field components of scattered laser radiation are generally elliptically polarized. Therefore, the level of the coefficient $\eta(\alpha_0, \Theta)$ becomes much lower, vanishing around $\tilde{J} = J^*$.

The choice of the optimal scattering angle Θ (with $\alpha_0 = \Delta\rho$) and the optimal polarization plane for scattering angles corresponding to the extreme situation, $\{\eta(\alpha_0, \Theta)\}|_{\Theta_i = \text{const}}$, is important for the photometry of the informative signal I^*. This is due to the fact that, when the extreme level $\eta(\alpha_0, \Theta) = \mu$ is achieved, the polarization structure of the informative signal varies for different α_0 and Θ (see Eqs. (4), (6), (8), and (9)).

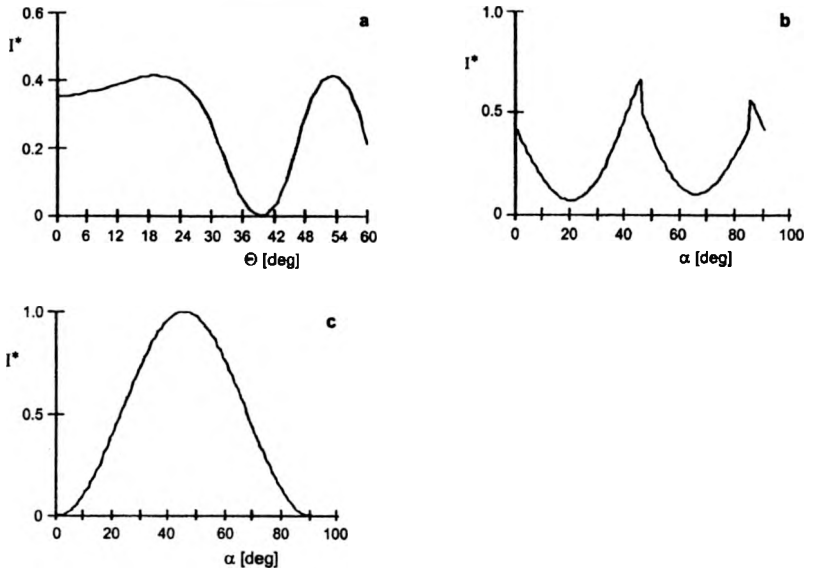

Fig. 3. Transfer function of the informative signal level: **a** – $\alpha = 20°$, **b** – $\theta = 35°$, **c** – $\theta = 55°$.

Figure 3 depicts a series of dependences of I^* calculated for the directions $\alpha_0 = 20°$ (Fig. 3**a**) and $\Theta = 35°$ (Fig. 3**b**), $\Theta = 55°$ (Fig. 3**c**) of extrema of the coefficient $\eta(\alpha_0, \Theta)$.

Analysing these results it can be seen that, when the minimum background level $\tilde{J} \times \mu^{-1}$ is achieved, the informative signal may vary within a broad dynamic range of three orders of magnitude (from 10^{-3} up to 1). An optimal photometric situation is achieved when the boundary conditions for the polarization state of the object signal produced by a biotissue (Eqs. (10)) are satisfied.

2.3. Experimental results

Figure 4 presents the results of experimental testing of the method of polarization laser probing of biotissues. Histological slices of biostructures placed in a sequence were employed as objects of studies. Optical and morphological parameters of these objects were correlated with the data of computer modeling. Experiments were performed with

– "cartilage–cancellous bony tissue" with $\Delta n_x = 0.1$, $\Delta n_y = 0.01$, $\Delta\rho \approx 20°$, $\alpha_0 = 20°$ (Fig. 4**a**) and $\Theta = 0°$ (Fig. 4**b**);

– "fibrillar muscular tissue–bony tissue" with $\Delta n_x = 0.1$, $\Delta n_y = 0.03$, $\Delta\rho \approx 20°$, $\alpha_0 = 20°$ (Fig. 4**c**), $\Theta = 0°$ (Fig. 4**d**), $\Theta = 35°$ (Fig. 4**e**), and $\Theta = 55°$ (Fig. 4**f**).

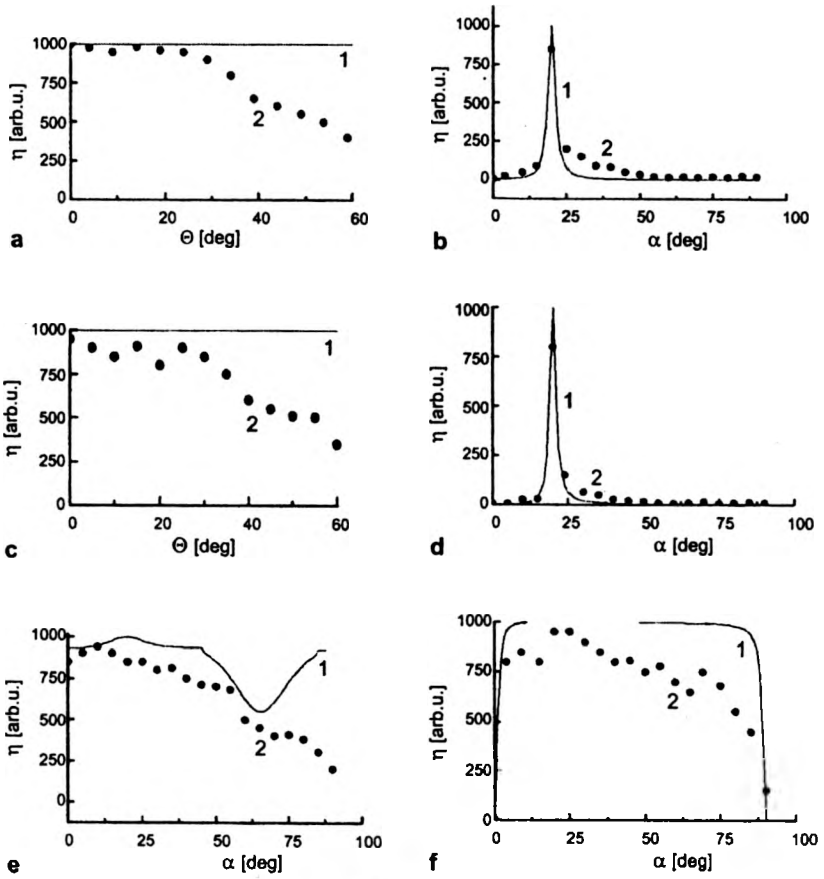

Fig. 4. Experimental dependences $\eta(\alpha_0, \Theta)$: **a** – "cartilage–cancellous bony tissue" with $\Delta n_x = 0.1$, $\Delta n_y = 0.01$, $\Delta\rho \approx 20°$ and $\alpha_0 \approx 20°$; **b** – "cartilage–cancellous bony tissue" with $\Delta n_x = 0.1$, $\Delta n_y = 0.01$, $\Delta\rho \approx 20°$ and $\Theta \approx 0°$; **c** – "fibrillar muscular tissue–bony tissue" with $\Delta n_x = 0.1$, $\Delta n_y = 0.03$, $\Delta\rho \approx 20°$ and $\alpha_0 \approx 20°$; **d** – "fibrillar muscular tissue–bony tissue" with $\Delta n_x = 0.1$, $\Delta n_y = 0.03$, $\Delta\rho \approx 20°$ and $\Theta \approx 0°$; **e** – "fibrillar muscular tissue–bony tissue" with $\Delta n_x = 0.1$, $\Delta n_y = 0.03$, $\Delta\rho \approx 20°$ and $\Theta \approx 35°$; **f** – "fibrillar muscular tissue–bony tissue" with $\Delta n_x = 0.1$, $\Delta n_y = 0.03$, $\Delta\rho \approx 20°$ and $\Theta \approx 55°$. 1 – theoretical results, 2 – experimental results.

The results of measurements of the coefficient $\eta(\alpha_0, \Theta)$ demonstrate the efficiency of polarization probing of biotissues within a sufficiently broad range of scattering angles, $\Theta < 0°$. The discrepancy between the results of computer modeling (solid lines in Fig. 4) and experimental data (points) does not exceed 10–20% within this range. As the observation angle Θ increases, the coefficient $\eta(\alpha_0, \Theta)$ noticeably decreases, while the discrepancy between theoretical predictions and experimental data may reach 50–80%. This effect is apparently due to the increase in the multiplicity of light scattering and the growth in the depolarization of the background signal, which is not included in theoretical modeling. However, even in this regime, the improvement factor of the signal-to-noise ratio remains sufficiently high, $\eta(\alpha_0, \Theta) \sim 10$–$100$.

3. Multiple scattering

3.1. Theoretical modeling

In the presence of a depolarized background component related to multiple light scattering, Eq. (1) can be rewritten as

$$\eta = \frac{\Pi[I^* + (I^* + \tilde{I})\mu]}{\Pi[I^* + (I^* + \tilde{I})\mu] + 0.5(1 - \Pi)(I^* + \tilde{I})} = \frac{I^*(1 + \mu) + \tilde{I}\mu}{\tilde{I}(1 + \mu + \omega) + I^*(\mu + \omega)} \tag{12}$$

where Π is the depolarization degree and $\omega = (1 - \Pi)/2\Pi$.

It can be seen from Eq. (12) that the depolarization parameter ω noticeably lowers the improvement factor of the signal-to-noise ratio in multiply scattering object scenes. This tendency is shown in Fig. 5, which illustrates the lowering in the improvement factor of the signal-to-noise ratio with a decrease in the polarization degree on a logarithmic scale. It follows from this figure that for $\Pi = 0.9$, the coefficient η is reduced by two orders of magnitude, while for $\Pi = 0.1$, the factor η decreases further virtually by another order of magnitude.

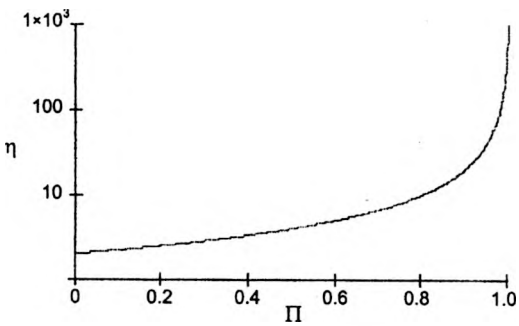

Fig. 5. Level of the signal-to-noise ratio as a function of the depolarization degree of the background signal.

On the other hand, the analysis of Eq. (1) shows that the improvement factor of the signal-to-noise ratio reaches its extreme level when both conditions of Eq. (10) are satisfied.

Such a situation can be implemented if the polarization state of the probing beam is determined in accordance with the following algorithm:

$$\alpha_0^* = 0.5 \arctan \frac{q_1 + \sqrt{q_1^2 - 4q_2q_3}}{2q_3},$$

$$q_1 = -[y_{32}(x_{33} + x_{22}) + x_{32}(y_{33} + y_{22})],$$

$$q_2 = x_{32}y_{23} + x_{22}y_{22},$$

$$q_3 = x_{23}y_{32} + x_{33}y_{33}, \tag{13}$$

$$\beta_0^* = -0.5 \arctan \frac{(x_{32} + x_{22})\cos 2\alpha_0^* + (x_{33} + x_{23})\sin 2\alpha_0^*}{x_{34} + x_{24}}. \quad (14)$$

Thus, correcting the polarization structure of a probing laser beam, one can increase the signal-to-noise ratio even under conditions of scattering with a high multiplicity.

3.2. Computer modeling

Figure 6 presents the results of computer modeling for the "spatial" and "topological" distributions of the improvement factor of the signal-to-noise ratio η obtained in the cases of single (Figs. 6**a**, **b**, $\Pi = 1.0$) and multiple (Figs. 6**c**, **d**, $\Pi = 0.12$) scattering and in the regime of polarization correction of the probing beam (Figs. 6**e**, **f**). Parameters of the object scene model a sequence of layers of cancellous bony and fibrillar muscular tissues with $\Delta n_x = 0.1$, $\Delta n_y = 0.03$, and $\Delta\rho = \rho_x - \rho_y = 0°$.

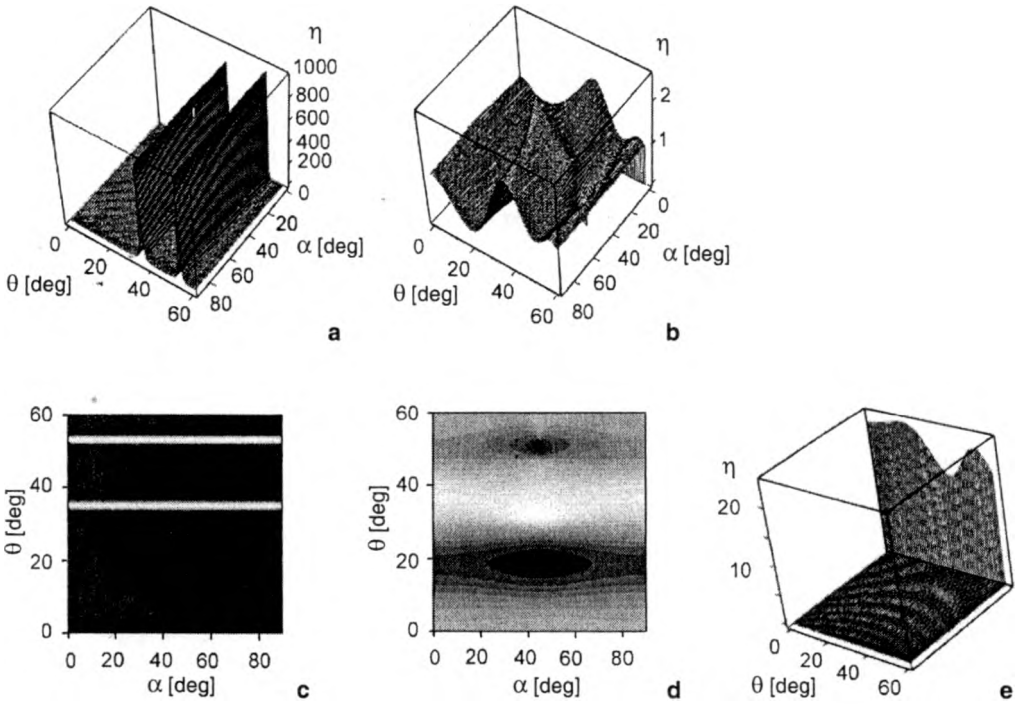

Fig. 6. Spatial-azimuthal and topological dependences of the improvement factor of the signal-to-noise ratio for singly and multiply scattering biostructures and in the regime of polarization correction of the probing beam **a, b** – the case of single scattering $\Pi = 1.0$; **c, d** – the case of multiple scattering $\Pi = 0.12$; **e** – the regime of polarization correction of probing beam.

The results of our modeling allow us to draw the following conclusions:

– In the regime of single scattering, the improvement factor of the signal-to-noise ratio reaches its extreme level ($\eta \to 10^3$) for the polarization azimuthal angles α_0 and

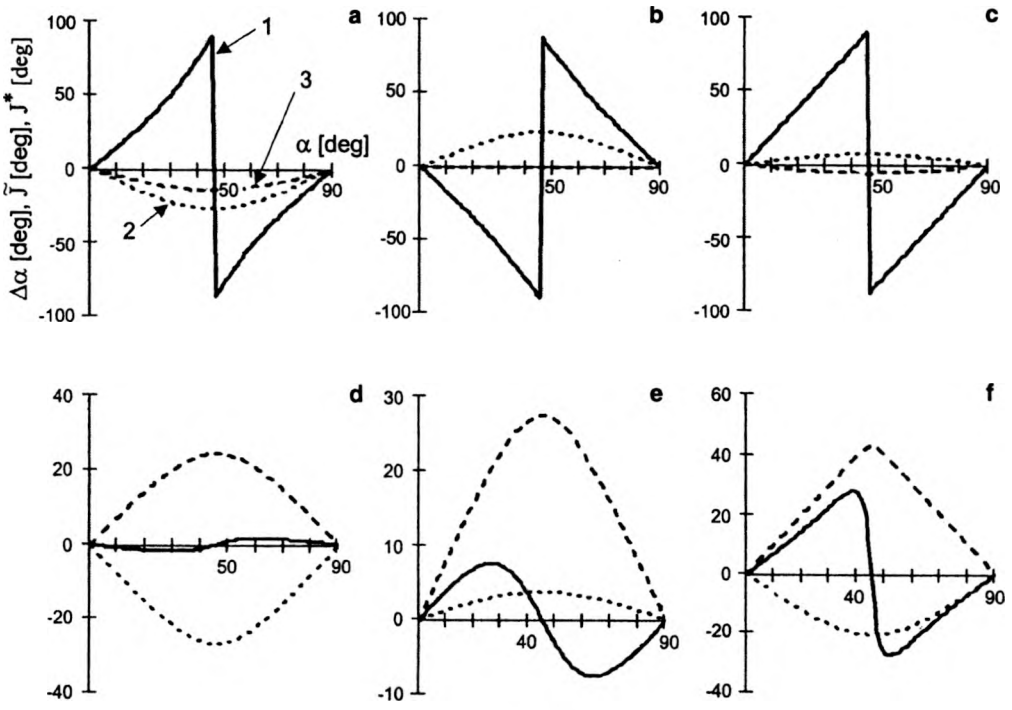

Fig. 7. Polarization structure of the background and informative signals: **a** – $\theta = 0°$, **b** – $\theta = 35°$, **c** – $\theta = 55°$, **d** – $\theta = 0°$, **e** – $\theta = 35°$, **f** – $\theta = 55°$ (1 – $\Delta\alpha$, 2 – J^*, 3 – $\tilde{J}$).

scattering angles Θ corresponding to a background signal whose vector structure tends to the structure of linearly polarized radiation ($\tilde{J} \to \min$), (Figs. 7**b**, **c**). Conversely, in the case where the informative and background signals are elliptically polarized ($J^* \to \max$, $\tilde{J} \to \max$), the coefficient ($\eta(\alpha_0, \Theta) \to \min$) tends to its minimum, vanishing in the limiting case, regardless of the difference of polarization azimuthal angles $\Delta\alpha$ (Fig. 7**a**).

– In the case of a multiply scattering muscular tissue, the level of η lowers by virtually three orders of magnitude within the entire range of azimuthal angles α_0 and angles Θ. This is due to the fact that the polarization states of the informative and background signals are virtually indistinguishable in this case, $\Delta\alpha \to \min$, $J^* \approx \tilde{J}$ (Figs. 7**d**–**f**).

– Polarization correction of the polarization state of a laser beam probing a multiply scattering object scene causes the improvement factor of the signal-to-noise ratio to increase by an order of magnitude for virtually any scattering angle Θ.

3.3. Experimental results

The results of experimental testing of the method of laser probing with a fixed polarization state and correction of the azimuth and ellipticity of polarization are presented in Fig. 8. Curves 1–3 obtained for the scattering angles $\Theta = 0°$, $\Theta = 20°$, and

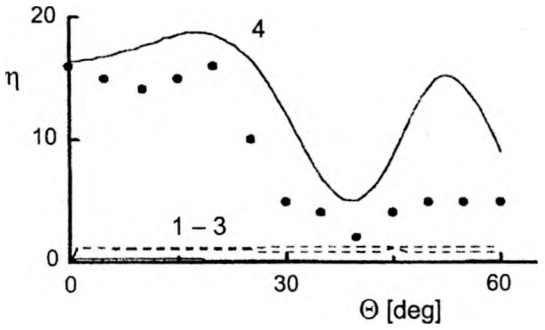

Fig. 8. Results of experimental testing of biotissues with a high level depolarized background signal: 1 – $\theta = 0°$, 2 – $\theta = 20°$, 3 – $\theta = 55°$, 4 – in the regime of polarization correction of probing beam.

$\Theta = 55°$, respectively, illustrate the efficiency of polarization probing of biotissues with a high level of the depolarized background signal. The results of laser probing with polarization correction are represented by curve 4.

The comparative analysis of the experimental data reveals the growth in the improvement factor of the signal-to-noise ratio by virtually an order of magnitude for any angle Θ.

A comparison with the results of analytical modeling shows a satisfactory agreement between theoretical predictions and experimental data. The level of discrepancies varies from 10 to 30%. Lower signal-to-noise ratios obtained in experiments may be due to some variance of orientations of optically active elements in bony and muscular tissues, which may increase the ellipticity of the object field [6], and a variance of the optical anisotropy of biotissues.

The results of the studies presented in this paper may be useful for the development of systems for polarization tomography and mammography oriented at early optical diagnostics of pathological changes in the morphological structure of biotissues.

References

[1] TUCHIN V.V., Proc. SPIE **1884** (1993), 234.

[2] ANGEL'SKII O.V., USHENKO A.G., ARKHELYUK A.D., ERMOLENKO S.B., BURKOVETS D.N., Kvantovaya Elektron. **29** (1999), 235 (in Russian).

[3] USHENKO A.G., Kvantovaya Elektron. **29** (1999), 239 (in Russian).

[4] USHENKO A.G., ERMOLENKO S.B., BURKOVETS D.N., USHENKO YU.A., Opt. Spektrosk. **87** (1999), 470 (in Russian).

[5] USHENKO A.G., BURKOVETS D.M., YERMOLENKO S.B., ARKHELUK A.D., PISHAK V.P., PISHAK O.V., WANCHULIAK O.Y., BACHINSKY V.T., GRIGORISHIN P.M., ZIMNAYAKOV D.A., Proc. SPIE **3904** (1999), 553.

[6] ANGELSKY, O.V., USHENKO, A.G., PISHAK, V.P., BURKOVETS D.M., YERMOLENKO S.B., PISHAK O.V., USHENKO YU.A., Proc. SPIE **4016** (1999), 413.

Received June 3, 2002